Anti-melanogenic effects of extracellular vesicles derived from plant leaves and stems in mouse melanoma cells and human healthy skin

Ruri Lee , Hae Ju Ko , Kimin Kim , Yehjoo Sohn , Seo Yun Min , Jeong Ah Kim , Dokyun Na & Ju Hun Yeon

View supplementary material

Published online: 18 Dec 2019.

Submit your article to this journal

Article views: 2356

View related articles

View Crossmark data

Citing articles: 4 View citing articles

Taylor & Francis
Taylor & Francis Group

RESEARCH ARTICLE

OPEN ACCESS | Check for updates

Anti-melanogenic effects of extracellular vesicles derived from plant leaves and stems in mouse melanoma cells and human healthy skin

Ruri Lee[a]*, Hae Ju Ko[a]*, Kimin Kim[a], Yehjoo Sohn[a], Seo Yun Min[b], Jeong Ah Kim[b], Dokyun Na[c] and Ju Hun Yeon[a]

[a]Department of Integrative Biosciences, University of Brain Education, Cheonan, Republic of Korea; [b]Biomedical Omics Group, Korea Basic Science Institute, Cheongju, Republic of Korea; [c]School of Integrative Engineering, Chung-Ang University, Seoul, Republic of Korea

ABSTRACT

Consumer interest in cosmetic industry products that produce whitening effects has increased demand for agents that decrease melanin production. Many such anti-melanogenic agents are associated with side effects, such as contact dermatitis and high toxicity, and also exhibit poor skin penetration. Considerable recent research has focused on plant-derived products as alternatives to chemotherapeutic agents that possess fewer side effects. In the current study, we investigated the anti-melanogenic effects of extracellular vesicles (EVs) extracted from leaves and stems of *Dendropanax morbifera*. Using spectrophotometric and biochemical approaches, we found that leaf-derived extracellular vesicles (LEVs) and stem-derived extracellular vesicles (SEVs) reduced melanin content and tyrosinase (TYR) activity in the B16BL6 mouse melanoma cell line in a concentration-dependent manner. An electron microscopy analysis further confirmed that LEVs and SEVs induce a concentration-dependent decrease in melanin content in melanoma cells. Both LEVs and SEVs exerted a greater whitening effect on melanoma cells than arbutin, used as a positive control, with LEVs producing the greater effect. Notably, neither LEVs nor SEVs induced significant cytotoxicity. We also examined the effects of plant-derived EVs on the expression of tyrosinase-related proteins (TRPs) in melanoma cells. LEVs inhibited expression of melanogenesis-related genes and proteins, including microphthalmia-associated transcription factor (MITF), TYR, TRP-1 and TRP-2. In a human epidermis model, LEVs exerted a stronger inhibitory effect on melanin production than arbutin. Collectively, our data suggest that LEVs from *D. morbifera* may be a novel candidate natural substance for use as an anti-melanogenic agent in cosmeceutical formulations.

Introduction

Melanin, a key component of the pigmentary systems of human hair, eyes and skin, is produced by melanocytes through a process called melanogenesis [1]. Abnormal accumulation of melanin causes dermatological problems such as freckles, solar lentigo and melasma, as well as cancer and vitiligo [2–5]. Therefore, regulating melanogenesis is a crucial strategy in the treatment of hyperpigmentary disorders [6]. For example, hydroquinone, a hydroxyphenolic chemical compound that interferes with TYR activity, is used as a skin-bleaching agent in the cosmetic industry. However, hydroquinone may cause side effects such as contact dermatitis and exogenous ochronosis [7–9]. Tretinoin is another synthetic agent that inhibits TYR activity, but its use is associated with a high frequency of oedema or irritation [10].

Given limitations of existing compounds, there has been growing interest in identifying alternative anti-melanogenic agents from natural sources, reflecting the fact that cosmetics derived from plants and herbs tend to be milder than synthetic compounds, more biodegradable and exhibit lower toxicity profiles [11]. Leaf extracts of *Dendropanax morbifera* have been shown to inhibit melanin production through direct effects on intracellular TYR activation and expression of enzymes involved in melanin biosynthesis [12]. Extracts of leaves from *Croton sublyratus* have been similarly shown to inhibit melanin content and cellular TYR activity through suppression of melanogenesis-associated transcription factor (MITF) and melanogenic enzymes [13]. In addition, the leaves of *Morus alba* show inhibitory effects on TYR activity and melanin formation in melan-a cells [14]. *p*-Coumaric acid of *Panax ginseng* leaves was identified as a major TYR inhibitor [15].

Although various plant compounds have been used in cosmeceutical formulations, their low solubility, low

---

*These authors contributed equally to this work.
ⓘ Supplemental data for this article can be accessed here.

affinity for their targets and modest whitening effects on skin have hampered progress in improving the therapeutic effects of plant-based cosmetics. This has motivated a search for new and promising technologies for improving the effectiveness of cosmeceuticals and bioactive compounds and the efficiency of their delivery to the skin [16,17]. For example, a number of nano-sized delivery technologies have been successfully developed, including nano-aloe vera for effective skincare [18], nano-quercetin for delaying ultraviolet (UV) radiation-induced cell damage [19], nano-fullerene for collagen regeneration and protection against skin ageing [20], nano-lutein for retention of antioxidant activity [21] and nano-resveratrol to protect the skin against UV radiation [22].

In this study, we focused on the effects of extracellular vesicles (EVs) derived from plants. It has recently been demonstrated that plant-derived EVs have a structure similar to that of exosomes isolated from mammals and act as extracellular messengers that mediate intercellular communication. In addition, these vesicles have been shown capable of transporting mRNAs, microRNAs (miRNAs), bioactive lipids and proteins to animal cells [23].

Here, we investigated the inhibitory effects of EVs derived from leaves and stems of *D. morbifera* on melanin production. Our analysis of the size and properties of leaf-derived extracellular vesicles (LEVs) and stem-derived extracellular vesicles (SEVs) extracted from *D. morbifera* leaves and stems showed that these EVs are readily taken up by melanoma cells and are not cytotoxic. To demonstrate the anti-melanogenic effect of LEVs and SEVs, we examined melanin content and TYR activity in melanoma cells. We further evaluated the effects of the EVs on melanin synthesis of complex process by monitoring changes in the levels of various proteins and enzymes [24].

α-Melanocyte-stimulating hormone (α-MSH) binds to MC1R (melanocortin-1 receptor) on the cell surface and activates adenylate cyclase, which leads to an elevated level of intracellular cyclic AMP (cAMP). cAMP is mediated through cAMP-dependent protein kinase A which results in the phosphorylation of cAMP response element-binding protein (CREB). Activated CREB induces MITF, which is expressed in melanocytes and is known to play a critical role in the differentiation and development of melanocyte. MITF regulates tyrosinase-related protein (TRP) family, which are multienzyme complexes including tyrosinase (TYR), Tyrp1 (TRP1) and Dct (TRP2). TYR activity is more stable in the presence of TRP-1 and TRP-2, and TYR is coexpressed with TRP1 or TRP2 by the regulation of MITF in melanoma cells [25]. TRP1 is a necessary enzyme for the correct trafficking of TYR to melanin synthesis, and TRP2 plays an important role in TRP catalytic activity in the early stages in melanin synthesis. All three interact with one another in melanoma cells (Supplementary Figure S1) [26–31].

We found that MITF expression was decreased followed by a reduction in TYR, TRP-1 and TRP-2 in melanoma cells treated with LEVs and confirmed that intracellular melanin synthesis was reduced at the ultrastructure level in these cells using electron microscopy. We further confirmed the anti-melanogenic effects of LEVs using a reconstituted human epidermis model. To quantitatively evaluate the anti-melanogenic effects of LEVs on cellular melanin synthesis in this model, we prepared standard solutions from tissues and measured melanin content using a Chroma Meter. Melanin spots were reduced in tissue sections stained with Fontana-Masson. LEVs inhibited the production of melanin more effectively than arbutin, a TYR inhibitor used as a positive control.

Collectively, these findings suggest that using natural substances-derived EVs for the treatment of hyperpigmentation is a viable future approach for the cosmeceutical industry. In addition, plant-derived EVs, which offer the multiple benefits of small size, low toxicity, high uptake and environmental safety, could serve as next-generation therapeutic delivery systems for the treatment of other diseases. Notably, the excellent anti-melanogenic effects of plant-derived EVs on reconstructed human skin tissue, which is similar to human epidermis, set the stage for future clinical trials.

Materials and methods

Isolation of D. morbifera LEVs and SEVs

Fresh leaves and stems of *D. morbifera* were collected from Bogildo, located in Wando-gun, Jeollanam-do, South Korea. EVs were isolated from 50 g of leaves and stems, respectively, by grinding with an extractor, passing the resulting juice through filter paper and centrifuging at $10,000 \times g$ for 10 min. Large debris was removed by filtering the supernatant through a 0.22-μm membrane, after which EVs were concentrated by centrifuging the sample at $5,000 \times g$ for 10 min at 4°C using an Amicon Ultra-4 PL 100 K centrifugal filter (Merck Millipore, Darmstadt, Germany). After centrifugation, the protein concentration of EVs was determined using a bicinchoninic acid (BCA) protein assay kit (Thermo Fisher Scientific, Waltham, MA, USA) [32].

Size characterization of isolated EVs

The hydrodynamic size of isolated EVs was measured by dynamic light scattering (DLS), a technique for determining the size-distribution profiles of small particles in suspension, using a Zetasizer nano ZS90 system (Malvern Instruments, Malvern, UK). Collected EVs were placed in a thermostatic cell at 20°C. The size distribution and z-average used for determining hydrodynamic size distribution were determined by measuring scattered intensity autocorrelation functions. Isolated EVs, diluted in vesicle-free water, were visualized and counted by nanoparticle tracking analysis (NTA) (Nanosight; Malvern Instruments) at a temperature of 25°C using a 488 nm laser.

Transmission electron microscopy analysis of EVs

For transmission electron microscopy (TEM) analysis, 5 μL of sample solution was loaded onto a copper-grid coated carbon film. After the sample had adsorbed for 1 min, the grid was washed with a drop of purified water and then negatively stained with 1% uranyl acetate for 1 min. Excess stain solution was removed using a piece of filter paper, and the grid was air-dried. The sample was imaged at a focus between 0.8 and 1.5 μm using a JEM-1400 Plus transmission electron microscope (JEOL Ltd., Tokyo, Japan) equipped with a Lab6 gun and operating at 120 kV. Images were recorded using an UltraScan OneView CMOS camera (Gatan, Pleasanton, CA, USA).

Preparation of liposomes

Liposomal formulations were prepared as lipid films using a 95:5 (mol/mol) ratio of DMPC (1,2-dimyristoyl-sn-glycero-3-phosphocholine) (Avanti Polar Lipids, Alabaster, AL, USA) to DSPE-mPEG (1,2-distearoyl-sn-glycero-3-phosphoethanolamine-N-[methoxy(polyethyleneglycol) −2000] (Avanti Polar Lipids). The hydrophobic fluorescent dye, 1,1-dioctadecyl-3,3,3′,3′-tetra-methylindocarbocyanine perchlorate (DiI, Invitrogen, Waltham, MA, USA) was mixed with EVs, 725.49 μg DMPC, 151.64 μg DSPE-PEG and 15 μg DiI. After evaporating organic solvent, the film containing the lipid and DiI mixture was hydrated with 1 mL of phosphate-buffered saline (PBS). Next, a liposome having a size of 100 nm was prepared using an extruder (Avanti Polar Lipids).

Cell culture and viability assays

B16BL6 melanoma cells were cultured in α-minimum essential media (α-MEM) (Gibco, Thermo Fisher Scientific) containing 10% foetal bovine serum (Rocky Mountain Biologicals, Missoula, MT, USA), and 1% penicillin/streptomycin (Lonza, Basel, Switzerland). The cells were cultured at 37°C in a humidified 5% CO_2 atmosphere. For cell viability assays, B16BL6 melanoma cells in a volume of 100 μL were seeded in 96-well plates (5×10^4 cells/well). After incubating for 24 h, cells were treated with 10 μL of LEVs and SEVs at 1, 5 and 10 μg/mL for 24 h, respectively. The concentrations of liposomes and arbutin were 10 and 70 μg/mL, respectively, in all experiments. Thereafter, 10 μL of EZ-Cytox reagent (Daeil Lab Service, Seoul, Korea) was added to each well and the plate was incubated for 1 h. The plate was then gently shaken before measuring absorbance at 450 nm using a microplate reader (BioTek, Winooski, VT, USA).

Cellular uptake assays

The internalization of EVs into cells was monitored by first staining LEVs and SEVs with lipophilic DiI (MOP-D-3911) (Invitrogen, Carlsbad, CA, USA). After treating cells with stained EVs for 1, 3, 6, 12, 24 and 48 h, growth medium was removed and the cells were fixed with 4% paraformaldehyde (Wako, Japan). Nuclei were then stained (blue) by adding Hoechst 33342 (Invitrogen) to the cells and incubating at room temperature (RT) for 15 min. Finally, the cells were washed with PBS containing 1% bovine serum albumin, and fluorescence (red and blue) was imaged under a fluorescence microscope (Leica Microsystems, Wetzlar, Germany). At least three fields were selected and analysed using ImageJ software.

Measurement of melanin content

For assessment of melanin content, B16BL6 melanoma cells were first seeded in 24-well plates (5×10^4 cells/well) in a volume of 500 μL. After incubating for 24 h, cells were treated with 100 nM α-MSH (Sigma-Aldrich, St. Louis, MO, USA) alone or with 50 μL of LEVs and SEVs at 1, 5 and 10 μg/mL for 48 h. Treated cells were washed with PBS and detached by incubating with 2.5% trypsin (Gibco, Thermo Fisher Scientific). The cell pellets were dissolved in a 1N NaOH solution (Sigma-Aldrich) containing 1% DMSO (Sigma-Aldrich) at 80°C for 1 h. Cell lysates were transferred to 96-well plates, and melanin content was determined by measuring absorbance at 405 nm using a microplate reader (BioTek). Melanin content was determined using a melanin standard curve constructed from 0 to 100 μg/mL of synthetic melanin solution (Sigma-Aldrich) dissolved in 1N NaOH (Supplementary

Figure S2). The melanin content was calculated by comparing with the control.

Tyrosinase activity assays

TYR activity was determined as L-DOPA oxidase activity. B16BL6 cells were cultured in 24-well plates at a density of 1×10^5 cells/well in α-MEM containing 100 nM α-MSH (Sigma-Aldrich) in a volume of 500 μL. After treating with 50 μL of LEVs and SEVs at 10, 50 and 100 μg/mL for 24 h, cells were washed with PBS and lysed with 1% Triton X-100 (Sigma-Aldrich). The lysed cells were freeze-thawed by incubation at −80°C for 30 min and then kept at RT for 10 min. The resulting samples were clarified by centrifugation at 12,000 × g for 15 min, after which 2 mg/mL of L-DOPA (Sigma-Aldrich) was added and the lysate was incubated at 37°C for 1 h. Absorbance was then measured at 490 nm using a microplate reader (BioTek).

Western blot analysis

Intracellular levels of proteins associated with anti-melanogenic pathways were determined by performing Western blot analyses on whole-cell extracts. B16BL6 murine melanoma cells in a volume of 500 μL were plated in 24-well plates (1×10^5 cells/well). Cell treated with EVs of 10, 50 and 100 μg/mL for 24 h in a volume of 50 μL were lysed by incubating in RIPA buffer (Thermo Fisher Scientific) for 20 min at 4°C in the presence of a protease inhibitor cocktail (Roche, Germany). Cell lysates were centrifuged for 15 min at 17,709 g, and protein concentration in the resulting lysates was measured using a BCA assay kit (Thermo Fisher Scientific). Equal amounts of protein (10–20 μg/sample) were loaded into wells of a Bolt 4–12% Bis-Tris Plus Gel (Invitrogen) and electro-transferred to a PVDF (polyvinylidene difluoride) membrane (GE Healthcare, Chicago, IL, USA). The membrane was rinsed with Tris-buffered saline containing 0.2% (v/v) Tween-20 (TBST), blocked in TBST containing 5% (w/v) skim milk (Gibco, Thermo Fisher Scientific) for 1 h at RT, and then incubated overnight at 4°C in primary antibody solutions diluted in TBST containing 1% (w/v) skim milk. Primary antibodies used included anti-TRP-1 (1:1000), anti-TRP-2 (1:1000) and anti-MITF (1:1000) antibodies from Abcam (Cambridge, England); and anti-TYR (1:500) antibody from Santa Cruz Biotechnology (Santa Cruz, CA, USA). Anti-β-actin antibody (1:500; Santa Cruz) was used for normalization of protein levels. Primary antibodies were detected using a species-appropriate horseradish per-oxidase (HRP)-conjugated secondary antibody, obtained from Genetex (Irvine, CA, USA). The membrane was rinsed with TBST and incubated for 1 h at RT with secondary antibody, diluted 1:2000 in TBST. The membrane was washed with TBST, and signals produced following incubation with enhanced chemi-luminescence (ECL) reagents (GE Healthcare) were detected using an ImageQuant 350 gel-imaging system (GE Healthcare).

Electron microscopy detection of intracellular melanin production

Cells were treated with LEVs or SEVs and incubated for 48 h. Treated cells were fixed by incubating with 200 mM cacodylate buffer containing 8% glutaralde-hyde and 20% paraformaldehyde (Wako). After dehydration with ethanol, ultrathin sections were prepared using a Leica EM UC7 microtome (Leica) and collected on 200 mesh copper grids. The sections were stained with 1% uranyl acetate and lead citrate, and images were obtained with a JEOL JEM 1010 transmission electron microscope (JEOL) at 80 kV.

Measurement of whitening effect using a human skin model

Neoderm-ME (Tego Science, Seoul, Korea), a human skin model, was used to examine the whitening effect of LEVs. Human skin tissue was treated with media as negative control or with 10 μg/mL of LEVs for 7 days. The concentration of arbutin was 70 μg/mL. The human skin tissue was dissolved in 1N NaOH and melanin content was determined by measuring the absorbance at 405 nm using a microplate reader (BioTek). On day 7, skin pigmentation was compared by microscopic analysis of Fontana-Masson–stained samples. For Fontana-Masson staining, skin samples were fixed in 4% paraformaldehyde (Waco) overnight at RT, sectioned and embedded in paraffin. Paraffin-embedded sections were then dried by heating in an oven at 60°C for 1 h. Slide-mounted sections were subsequently dehydrated by immersing three times in xylene, two times in 95% ethanol and two times in 100% ethanol, and then washed with distilled water. Fontana-Masson staining was performed using ammoniacal silver solution at 56°C and washed with distilled water. The slides were then fixed by incubating in a 0.2% gold chloride solution at RT and immersed in 5% sodium thiosulphate solution at room RT. Finally, slides were dehydrated in fresh alcohol.

Statistical analysis

Data obtained from the experiment were presented as mean ± SEM. We have done the experiments about viability, melanin content and TYR activity in four batches (Supplementary Figure S3). Statistical analysis was performed using one-way analysis of variance (ANOVA) and Dunnett's test with GraphPad Prism (GraphPad Prism Software Inc., San Diego, CA, USA). Differences at $p < 0.05$, $p < 0.01$, and $p < 0.001$ were considered statistically significant.

Results

Characterization of plant-derived EVs

To investigate EVs in the leaves and stems of *D. morbifera*, we extracted the juices from harvested leaves and stems, and then isolated plant-derived EVs by filtration. The size distribution of EVs was measured using DLS and the concentration of nanoparticles was determined by NTA. The average diameter of EVs extracted from leaves (LEVs) and stems (SEVs) was

~90 nm, and the total number of LEVs and SEVs isolated from 50 g of leaves and stems was 1.53×10^9 particles/g and 4.98×10^8 particles/g, respectively. TEM images revealed that LEVs and SEVs were nearly circular and varied in size (30–200 nm), findings consistent with DLS and NTA results (Figure 1(a,b)).

Cellular uptake of plant-derived EVs into melanoma cells

To quantitatively evaluate the cellular uptake of plant EVs into melanoma cells, we treated B16BL6 murine melanoma cells with LEVs at different concentrations and for different lengths of time. LEVs and nuclei were stained with DiI (red) and Hoechst 33324 (blue), respectively. As shown in Figure 2, treatment of melanoma cells for 48 h with different concentrations of 1, 5 or 10 μg/mL of LEVs and SEVs resulted in a time-dependent and concentration-dependent increase in cellular uptake. LEVs and SEVs were widely distributed throughout the cytoplasm surrounding the nucleus (Figure 2(a,c)). The uptake of LEVs at 1 μg/mL was
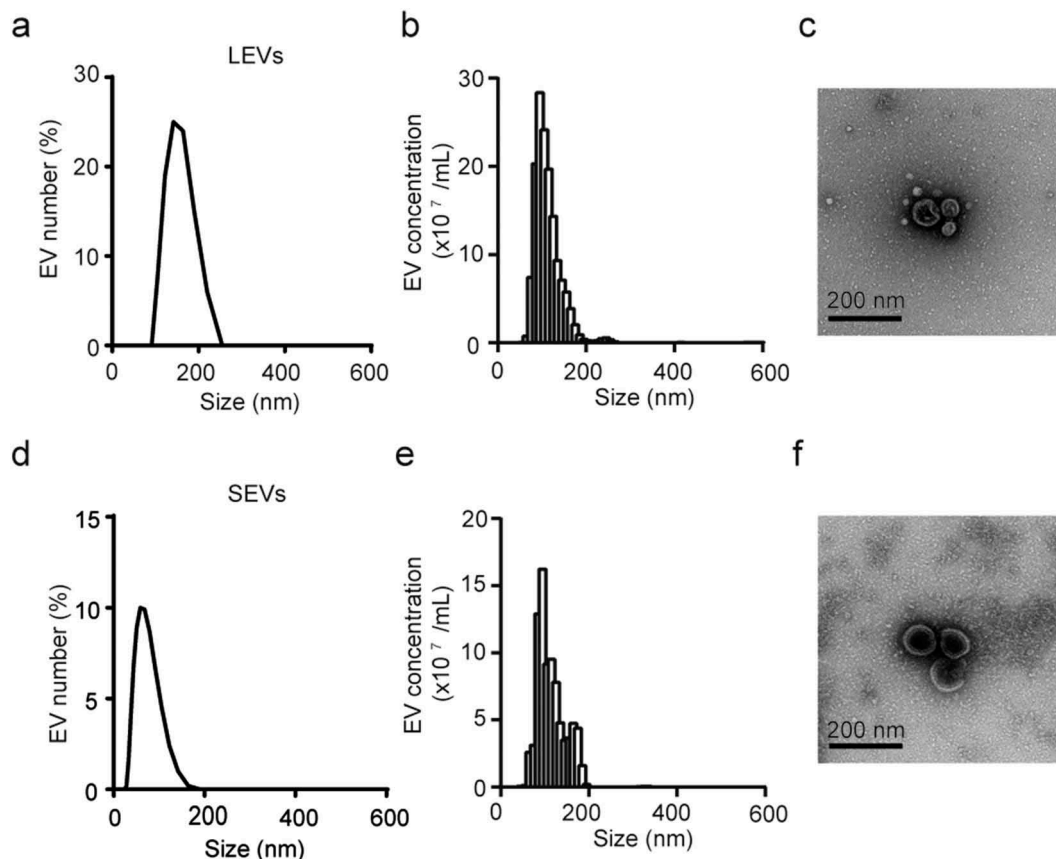

Figure 1. Characterization of LEVs and SEVs from *D. Morbifera*.
Size distribution and concentration of LEVs, determined by (a) DLS and (b) nanoparticle tracking analysis (NTA) measurement. (c) Transmission electron microscopy (TEM) image of LEVs. Size distribution concentration of SEVs, determined by (d) DLS and (e) nanoparticle tracking analysis (NTA) measurement. (f) Transmission electron microscopy (TEM) image of SEVs. Scale bars: 200 nm.
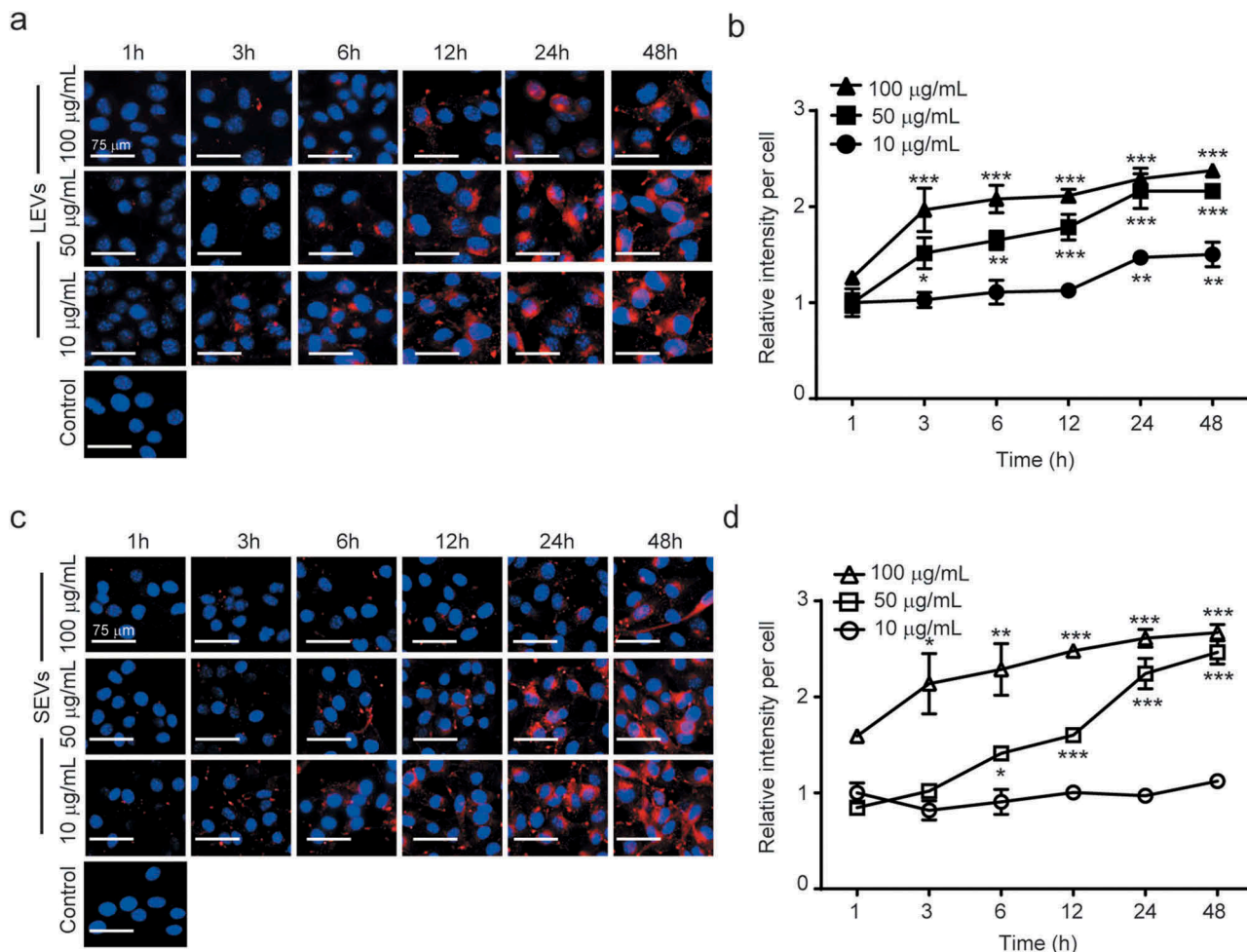
Figure 2. Cellular uptake of plant-derived EVs and viability of melanoma cells.

(a) Representative fluorescence microscope images of cellular uptake of LEVs at 1, 5 and 10 µg/mL. Scale bars: 75 µm. (b) Quantification of the uptake of LEVs up to 48 h. (c) Representative fluorescence microscope images of cellular uptake of SEVs at 1, 5 and 10 µg/mL. Scale bars: 75 µm. (d) Quantification of the uptake of SEVs up to 48 h. *, ** and *** indicate difference for $p < 0.05$, $p < 0.01$ and $p < 0.001$ in comparison to the cells treated with cell culture media as negative control, respectively. (n = 3).

saturated after 24 h, LEVs at 5 and 10 µg/mL were rapidly absorbed within 3 h and saturated after 12 h (Figure 2(b)). Also, 5 and 10 µg/mL of SEVs were gradually transferred to the cells for 6 h and saturated after 24 h (Figure 2(d)).

To verify the cytotoxic effect of LEVs and SEVs, we treated murine melanoma B16BL6 cells with 1, 5 or 10 µg/mL of EVs for 24 h and assessed their viability. As shown in Supplementary Figure S4, cell viability was maintained above 90%, even following treatment with 10 µg/mL of EVs. Therefore, we selected 10 µg/mL as an optimal concentration of plant-derived EVs and 24 h after treatment the optimal time for measuring absorption.

Inhibitory effects of EVs on melanin content and tyrosinase activity

We next examined the effect of LEVs and SEVs on melanin production and TYR activity in mouse melanoma B16BL6 cells. Melanin production in melanoma cells was stimulated by pre-treatment with α-MSH, and changes in melanin synthesis were observed after culturing with LEVs and SEVs for 48 h. Arbutin, a known TYR inhibitor, was used as a positive control. Both LEVs and SEVs induced concentration-dependent decreases in melanin production. This anti-melanin effect was significant at a concentration of 5 µg/mL for both EVs and was maximal at 10 µg/mL; at this higher concentration, LEVs and SEVs decreased melanin content by 48% and 34%, respectively (Figure 3(a)).

To confirm TYR inhibition by LEVs and SEVs in B16BL6 cells, we analysed TYR activity by measuring L-DOPA oxidase activity. LEVs affected to TYR activity less than 10% at 1 or 5 µg/mL, but LEVs at a concentration of 10 µg/mL reduced cellular TYR activity by 34% compared with negative controls (liposomes). Interestingly, SEVs showed only 10% TYR inhibition at all concentrations (Figure 3(b)).
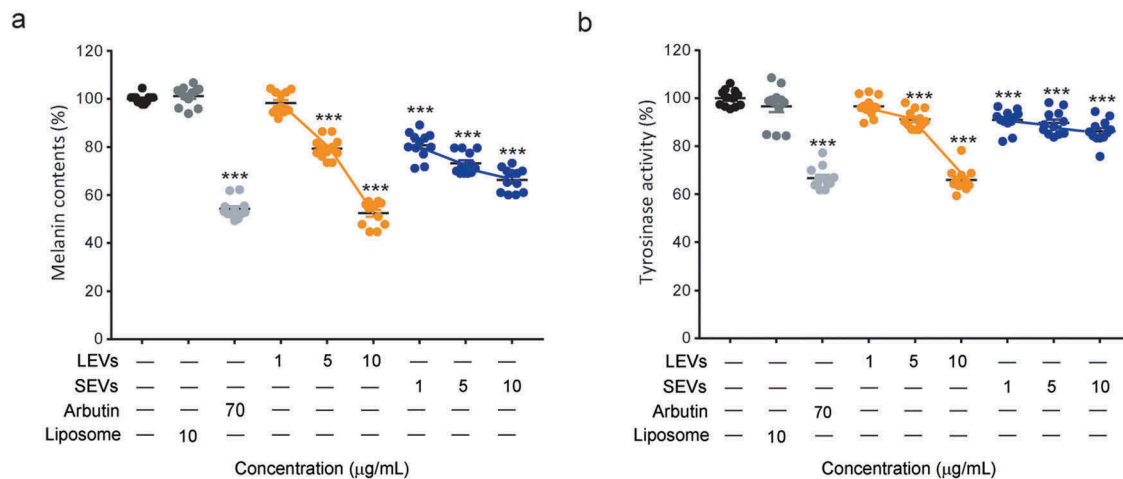
Figure 3. Melanin content and tyrosinase activity of B16BL6 murine melanoma cells.

Inhibition effect of melanin content on B16BL6 murine melanoma cells treated with LEVs or SEVs at 1, 5 and 10 μg/mL for 48 h. (a) melanin content inhibited by LEVs and SEVs. Inhibition effect of TYR activity on B16BL6 murine melanoma treated with LEVs or SEVs at 1, 5 and 10 μg/mL for 24 h. (b) TYR activity in melanoma cells treated with LEVs or SEVs. Melanin content and TYR activity were applied. *, ** and *** indicate difference for $p < 0.05$, $p < 0.01$ and $p < 0.001$ in comparison to the cells treated with cell culture media as negative control. The cells treated with arbutin were used as a positive control ($n = 12$).

Collectively, these results indicate that LEVs inhibit melanin production better than SEVs and reduced the associated TYR activity, effects similar to those of arbutin.

To verify the effect of LEVs and SEVs on melanin production by melanocytes and assess cell morphology, we also compared the ultrastructure of cells using TEM. As shown, untreated cells produced a relatively large amount of melanin around the nucleus and showed no significant change in morphology compared with controls (Figure 4(a–e)). In contrast, treatment with LEVs or SEVs caused a concentration-dependent decrease in melanin production. Specifically, both LEVs and SEVs reduced melanin formation by 67% and 60%, respectively, compared with the control (Figure 4(f,g)) and showed similar effects to arbutin when treated with 10 μg/mL of LEVs and SEVs (Figure 4(c)). These results suggest that *D. morbifera*-derived EVs have anti-melanin effects similar to those of arbutin.

Expression of melanogenesis-related proteins in melanoma cells

Along with the α-MSH-MC1R pathway, MITF-target genes including TYR, TRP-1 and TRP-2 regulate melanocyte pigmentation [26]. To study the mechanisms by which LEVs regulate melanin production, we measured the expression level of each of these proteins by Western blot analysis. SEVs were excluded from these analyses because 10 μg/mL of SEVs showed only 10% inhibition in TRY activity, while 10 μg/mL of LEVs and

arbutin showed 66% and 67% efficacy in TRY inhibition, respectively, so we focused on the effect of LEVs on protein expression (Figure 3(b)).

Bl6BL6 melanoma cells stimulated with α-MSH were treated with 1, 5 or 10 μg/mL of LEVs and the relative expression levels of MITF, TYR, TRP-1 and TRP-2 protein were measured. As shown in Figure 5 (a), LEVs caused a concentration-dependent decrease in MITF levels, reducing protein expression by 29% and 58% at 5 and 10 μg/mL, respectively.

As shown in Figure 5(b), LEVs induced a concentration-dependent decrease in TYR protein expression, reducing it by 60% and 43% at 5 and 1 μg/mL, respectively. At a concentration of 10 μg/mL, LEVs also decreased the expression levels of TRP-1 and TRP-2 by 35% and 27%, respectively (Figure 5(c,d)).

Inhibitory effect of LEVs on melanin synthesis in human skin tissue

To confirm the inhibitory effect of plant-derived EVs on melanogenesis in human skin, we treated a 3-dimensional, reconstituted human epidermis model composed of human melanocytes and keratinocytes with 10 μg/mL of LEVs and compared the results to those obtained with arbutin. After 7 days of treatment, LEVs-treated tissues and pellets obtained from them were found to be lighter than human skin tissue treated with culture media as negative control (Figure 6(a)). Images of Fontana-Masson–stained tissue sections indicated that the melanin distribution in the epidermis was reduced by LEVs (Figure 6(b)), suggesting that these EVs would
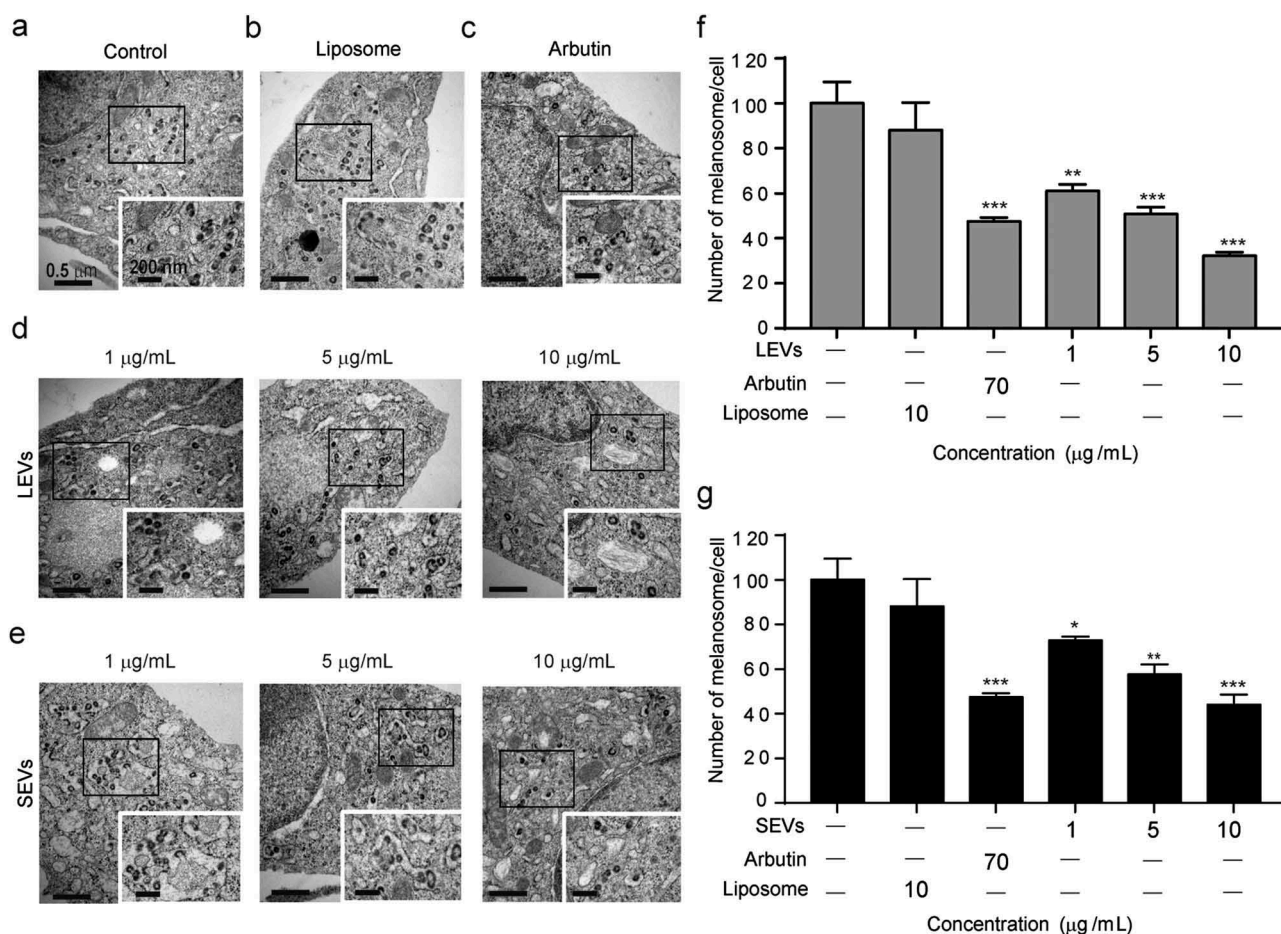
Figure 4. Electron microscopy detection of intracellular melanin production.

Changes of melanin content in melanoma cells with (a) no treat, (b) 10 μg/mL of liposome, (c) 70 μg/mL of arbutin, (d) 1, 5 and 10 μg/mL of LEVs and (e) 1, 5 and 10 μg/mL of SEVs. Scale bars: 0.5 μm (left) and 200 nm (right). (f) Quantification of melanin production in cells treated with LEVs. (g) Quantification of melanin production in cells treated with SEVs. *, ** and *** indicate difference for $p < 0.05$, $p < 0.01$ and $p < 0.001$ in comparison to the cells treated with cell culture media as negative control. The cells treated with arbutin were used as a positive control (n = 3).

exert a noticeable whitening effect on human skin. The difference in lightness value, indicating the brightness of the skin, was measured using a chromameter. The brightness of skin treated with LEVs was significantly higher than that of controls, and notably was also higher than that of skin treated with arbutin (Figure 6(c)). A quantitative analysis of melanin content of lysed human skin cells after treatment with LEVs showed a decrease of 43% and 28% compared to the untreated negative control and arbutin as a positive control (Figure 6(d)). A microscopic analysis of the tissues showed 29% and 26% reduction by LEVs and arbutin treatment compared to the untreated negative control in the degree of pigmentation (Figure 6(e)).

Discussion

Unlike most eukaryotic cells, plants have complex cell walls that constitute a significant barrier to the movement of exosomes. Therefore, exosomes released from plant cells pass through a series of fusions of multivesicular bodies with the plasma membrane. The secretory products released by the plant secretions are deposited in a periplasmic space adjacent to the plasma membrane; as they accumulate, they create a pressure that permits a flux of secretions across the cell wall barrier. Thus, secreted substances, including exosomes, can be released without an energy requirement [33–35]. The size of plant-derived EVs was similar to or larger than that of naturally occurring animal cell exosomes, and was similar to that observed for sunflower apoplastic fluids (50–200 nm) and EVs derived from *Arabidopsis rosette* (50–300 nm) [36,37]. The efficiency of cellular uptake is considered a key factor in determining therapeutic efficacy because the targets of many therapeutic agents are located in intracellular compartments [38]. Therefore, we identified the optimal time and concentration for the absorption by melanoma
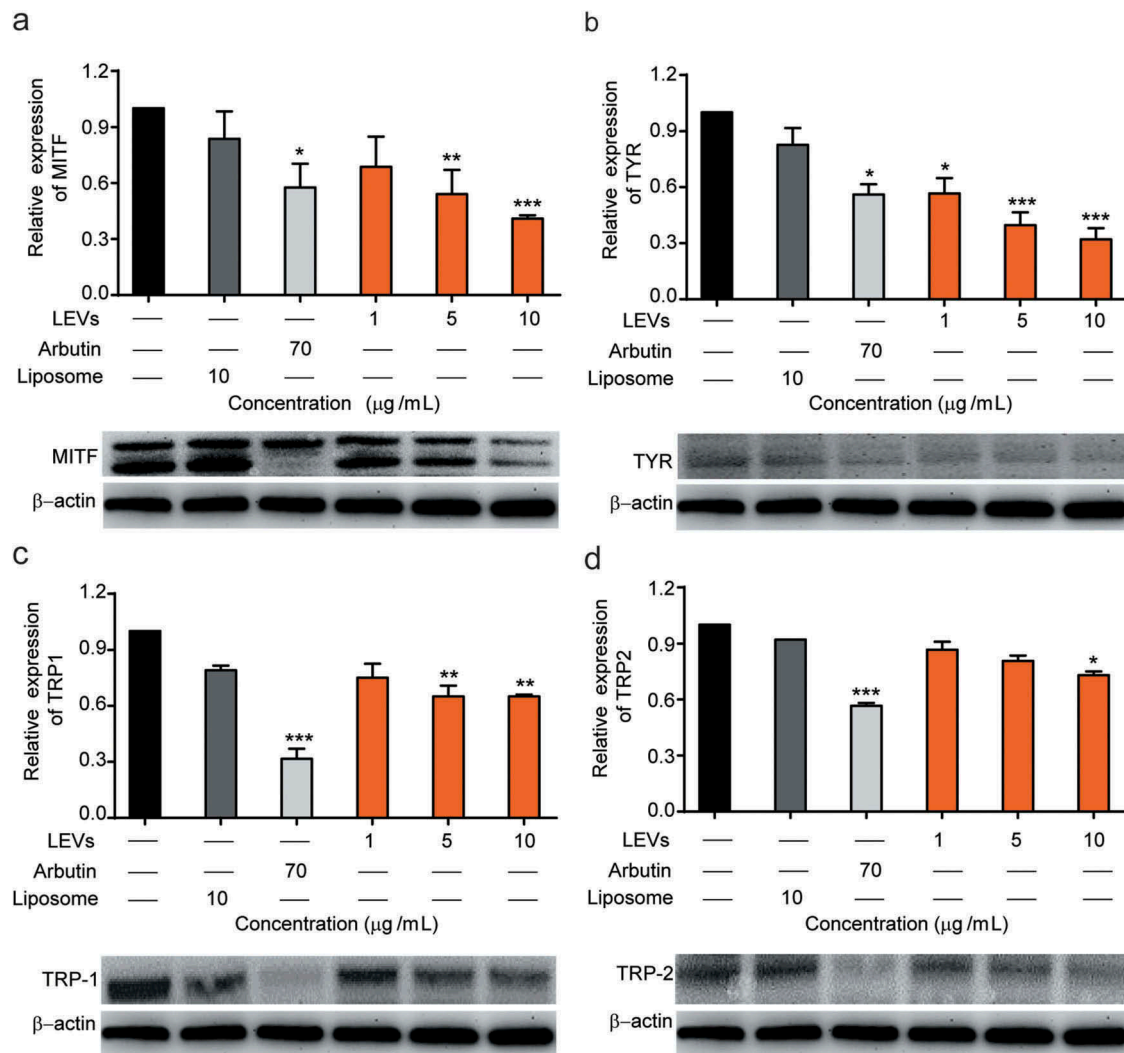
Figure 5. Expression levels of melanogenesis-related proteins in B16BL6 murine melanoma cells.

Western blot analysis performed on B16BL6 murine melanoma cells treated with LEVs at 1, 5 and 10 µg/mL for 24 h. (a) Effect of LEVs on MITF protein levels. (b) Effect of LEVs on TYR protein levels. (c) Effect of LEVs on TRP-1 protein levels. (d) Effect of LEVs on TRP-2 protein levels Western blot analysis were applied. *, ** and *** indicate difference for $p < 0.05$, $p < 0.01$ and $p < 0.001$ in comparison to the cells treated with cell culture media as negative control. The cells treated with arbutin were used as a positive control (n = 3).

cells and observed that both LEVs and SEVs were rapidly transferred to melanoma cells within 12 h.

TYR is a glycoprotein that catalyzes the conversion of L-tyrosinase into L-DOPA, the rate-limiting step in melanin synthesis [39]. Both EVs showed anti-melanogenic effects, but the effects of LEVs were clearly greater than those of SEVs.

Melanin production is regulated by α-MSH-MC1R, and it is known that inhibition of PKC reduces skin and hair pigmentation [40,41]. However, a number of genetic, biochemical and pharmacological studies have demonstrated that α-MSH-MC1R signalling is the major driver of melanogenesis [26,42]. Though our experiments did not show a direct interaction between MITF and TYR, but proved that LEVs decrease the expression of TYR, TRP-1 and TRP-2 by reducing the

expression of MITF via the UV-dependent α-MSH-MC1R pathway in melanoma cells, and thereby inhibit melanogenesis. We assume that TRP family proteins are indirectly connected with each other, but further experiment might be required to prove direct interaction between them. Furthermore, the reconstructed human skin model exhibited the UV-induced melanin synthesis and melanin content was effectively inhibited by LEVs.

Conclusion

Our findings suggest that LEVs are candidates for new anti-melanogenic agents that reduce melanin production by inhibiting the expression of melanin-related proteins. The results confirm that LEVs
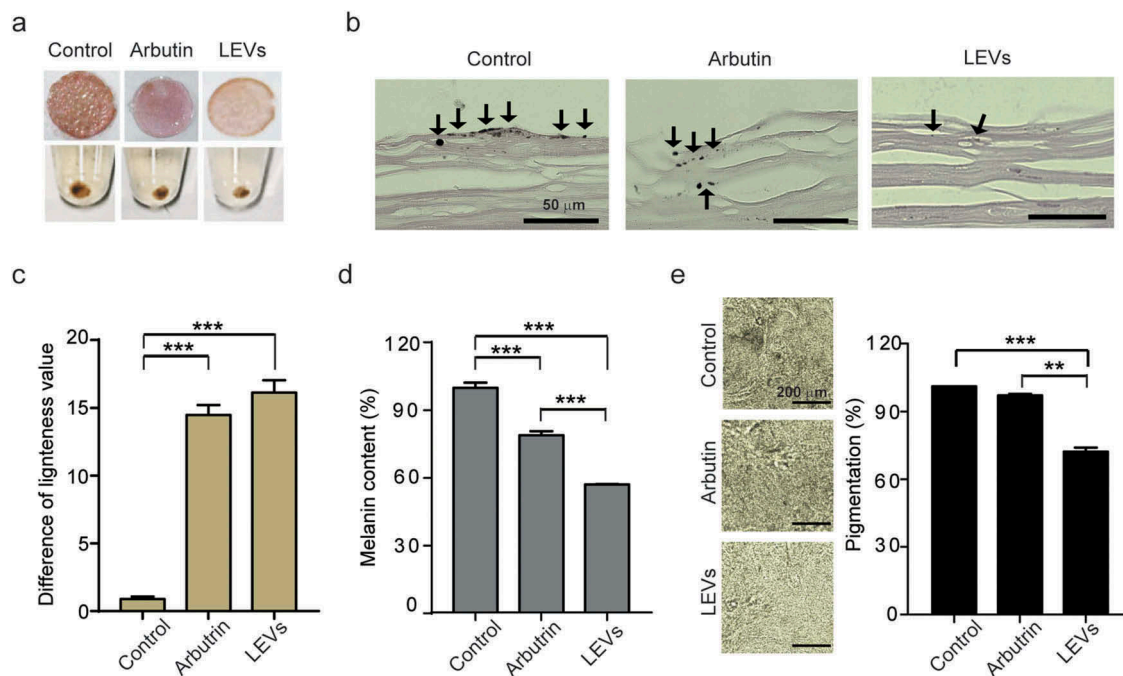
Figure 6. Whitening effect of LEVs on human skin tissue.
Reconstituted human epidermis model composed of human melanocytes and keratinocytes. (a) Representative images of cultured human skin tissue (top) and melanin pellets (bottom). (b) Images of human tissue sections stained with Fontana-Masson (FM). Scare bars: 50 μm. (c) Differences in lightness values, determined using a Chroma Metre. (d) Melanin content of human skin tissue. (e) Representative microscopic images of human skin tissue (left) and darkness of skin tissue, analysed by Image J software (right). Human skin tissue were applied. *, ** and *** indicate difference for $p < 0.05$, $p < 0.01$ and $p < 0.001$ in comparison to the human skin tissue treated with cell culture media as negative control. The human skin tissue treated with arbutin was used as a positive control (n = 3).

reduce MITF, which downregulates TRPs in B16BL6 melanoma cells. LEVs and arbutin showed 66% and 67% efficacy in TRY inhibition, respectively, and reconstituted human skin treated with LEVs showed 43% and 28% decrease in melanin content compared to the untreated negative control and arbutin as a positive control.

From the earlier results, we propose that plant-derived EVs can act as an anti-melanogenic agent to contribute to the development of natural cosmetics. Further research is needed to develop plant-derived EVs as an effective ingredient for skin improvement, and it is necessary to demonstrate the safety of plant-derived EVs using human skin models. Our results indicate that EVs can be used to reduce melanin and thereby to brightening skins. However, the EVs may have a toxic effect on skin, other additional experiments such as allergic test or Ames test should be carried out as well.

Acknowledgement

Disclosure of statement

No potential conflict of interest was reported by the authors.

Funding

References

[1] Meredith P, Sarna T. The physical and chemical properties of eumelanin. Pigment Cell Res. 2006;19(6):572–594.
[2] Grimes PE. Melasma: etiologic and therapeutic considerations. Arch Dermatol. 1995;131(12):1453–1457.
[3] Todd MM, Rallis TM, Gerwels JW, et al. A comparison of 3 lasers and liquid nitrogen in the treatment of solar lentigines: a randomized, controlled, comparative trial. Arch Dermatol. 2000;136(7):841–846.
[4] Kawalek AZ, Spencer JM, Phelps RG. Combined excimer laser and topical tacrolimus for the treatment of vitiligo: a pilot study. Dermatol Surg. 2004;30(2):130–135.
[5] Bastiaens M, Ter Huurne J, Gruis N, et al. The melanocortin-1-receptor gene is the major freckle gene. Hum Mol Genet. 2001;10(16):1701–1708.
[6] Pillaiyar T, Manickam M, Jung SH. Downregulation of melanogenesis: drug discovery and therapeutic options. Drug Discov Today. 2017;22(2):282–298.

[7] Hu ZM, Zhou Q, Lei TC, et al. Effects of hydroquinone and its glucoside derivatives on melanogenesis and anti-oxidation: biosafety as skin whitening agents. J Dermatol Sci. 2009;55(3):179–184.

[8] Westerhof W, Kooyers T. Hydroquinone and its analogues in dermatology–a potential health risk. J Cosmet Dermatol. 2005;4(2):55–59.

[9] Picardo M, Carrera M. New and experimental treatments of cloasma and other hypermelanoses. Dermatol Clin. 2007;25(3):353–362.

[10] Shin JW, Park KC. Current clinical use of depigmenting agents. Dermatol Sin. 2014;32(4):205–210.

[11] Chaita E, Lambrinidis G, Cheimonidi C, et al. Anti-melanogenic properties of Greek plants. A novel depigmenting agent from Morus alba wood. Molecules. 2017;22(4):1–14.

[12] Park SA, Park J, Park CI, et al. Cellular antioxidant activity and whitening effects of Dendropanax morbifera leaf extracts. Microbiol Biotechnol Lett. 2013;41(4):407–415.

[13] Chatatikun M, Yamauchi T, Yamasaki K, et al. Anti melanogenic effect of Croton roxburghii and Croton sublyratus leaves in α-MSH stimulated B16F10 cells. J Tradit Complement Med. 2019;9(1):66–72.

[14] Lee SH, Choi SY, Kim H, et al. Mulberroside F isolated from the leaves of Morus alba inhibits melanin biosynthesis. Biol Pharm Bull. 2002;25(8):1045–1048.

[15] Lim JY, Ishiguro K, Kubo I. Tyrosinase inhibitory p-Coumaric acid from Ginseng leaves. Phytother Res. 1999;13(5):371–375.

[16] Chanchal D, Swarnlata S. Novel approaches in herbal cosmetics. J Cosmet Dermatol. 2008;7(2):89–95.

[17] Ganesan P, Choi DK. Current application of phytocompound-based nanocosmeceuticals for beauty and skin therapy. Int J Nanomedicine. 2016;11 (11):1987–2007.

[18] Takahashi M, Kitamoto D, Asikin Y, et al. Liposomes encapsulating Aloe vera leaf gel extract significantly enhance proliferation and collagen synthesis in human skin cell lines. J Oleo Sci. 2009;58(12):643–650.

[19] Bose S, Du Y, Takhistov P, et al. Formulation optimization and topical delivery of quercetin from solid lipid based nanosystems. Int J Pharm. 2013;441(30):56–66.

[20] Ngan CL, Basri M, Tripathy M, et al. Skin intervention of fullerene-integrated nanoemulsion in structural and collagen regeneration against skin aging. Eur J Pharm Sci. 2015;70(5):22–28.

[21] Mitri K, Shegokar R, Gohla S, et al. Lipid nanocarriers for dermal delivery of lutein: preparation, characterization, stability and performance. Int J Pharm. 2011;414 (1–2):267–275.

[22] Juškaitė V, Ramanauskienė K, Briedis V. Design and formulation of optimized microemulsions for dermal delivery of resveratrol. Evid Based Complement Alternat Med. 2015;2015:1–10.

[23] Zhang M, Viennois E, Xu C, et al. Plant derived edible nanoparticles as a new therapeutic approach against diseases. Tissue Barriers. 2016;4(2):1–9.

[24] Criton M, Le Mellay-Hamon V. Analogues of N-hydroxy-N′-phenylthiourea and N-hydroxy-N′-phenylurea as inhibitors of tyrosinase and melanin formation. Bioorg Med Chem Lett. 2008;18 (12):3607–3610.

[25] Kobayashi T, Hearing VJ. Direct interaction of tyrosinase with Tyrp1 to form heterodimeric complexes in vivo. J Cell Sci. 2007;120(24):4261–4268.

[26] D'Mello S, Finlay G, Baguley B, et al. Signaling pathways in melanogenesis. Int J Mol Sci. 2016;17(7):1–18.

[27] Fang D, Tsuji Y, Setaluri V. Selective down-regulation of tyrosinase family gene TYRP1 by inhibition of the activity of melanocyte transcription factor, MITF. Nucleic Acids Res. 2002;30(14):3096–3106.

[28] Oh MJ, Hamid MA, Ngadiran S, et al. Ficus deltoidea (Mas cotek) extract exerted anti-melanogenic activity by preventing tyrosinase activity in vitro and by suppressing tyrosinase gene expression in B16F1 melanoma cells. Arch Dermatol Res. 2011;303(3):161–170.

[29] Jang EJ, Shin Y, Park HJ, et al. Anti-melanogenic activity of phytosphingosine via the modulation of the microphthalmia-associated transcription factor signaling pathway. J Dermatol Sci. 2017;87(1):19–28.

[30] Toyofuku K, Wada I, Valencia JC, et al. Oculocutaneous albinism types 1 and 3 are ER retention diseases: mutation of tyrosinase or Tyrp1 can affect the processing of both mutant and wild-type proteins. Faseb J. 2001;15:2149–2161.

[31] Xue L, Li Y, Zhao B, et al. TRP-2 mediates coat color pigmentation in sheep skin. Mol Med Rep. 2018;17:5869–5877.

[32] Mu J, Zhuang X, Wang Q, et al. Interspecies communication between plant and mouse gut host cells through edible plant derived exosome-like nanoparticles. Mol Nutr Food Res. 2014;58(7):1561–1573.

[33] Nosanchuk JD, Nimrichter L, Casadevall A, et al. A role for vesicular transport of macromolecules across cell walls in fungal pathogenesis. Commun Integr Biol. 2008;1(1):37–39.

[34] Robinson DG, Ding Y, Jiang L. Unconventional protein secretion in plants: a critical assessment. Protoplasma. 2016;253(1):31–43.

[35] Paiva EA. How do secretory products cross the plant cell wall to be released? A new hypothesis involving cyclic mechanical actions of the protoplast. Ann Bot. 2016;117(4):533–540.

[36] Hood JL, Scott MJ, Wickline SA. Maximizing exosome colloidal stability following electroporation. Anal Biochem. 2014;448(1):41–49.

[37] Rutter BD, Innes RW. Extracellular vesicles isolated from the leaf apoplast carry stress-response proteins. Plant Physiol. 2017;173(1):728–741.

[38] Luan X, Sansanaphongpricha K, Myers I, et al. Engineering exosomes as refined biological nanoplatforms for drug delivery. Acta Pharmacol Sin. 2017;38(6):754–763.

[39] Videira IF, Moura DF, Magina S. Mechanisms regulating melanogenesis. An Bras Dermatol. 2013;88(1):76–83.

[40] Park HY, Lee J, Kapasi S, et al. Topical application of a protein kinase C inhibitor reduces skin and hair pigmentation. J Invest Dermatol. 2004;122(1):159–166.

[41] Yamanishi DT, Graham M, Buckmeier JA, et al. The differential expression of protein kinase C genes in normal human neonatal melanocytes and metastatic melanomas. Carcinogenesis. 1991;12(1):105–109.

[42] Borovansky J, Riley PA. Melanins and melanosomes: biosynthesis, biogenesis, physiological, and pathological functions. Hoboken, NJ: Wiley-Blackwell; 2011.